JOURNAL OF OPTOELECTRONICS AND ADVANCED MATERIALS Vol. 12, No. 10, October 2010, p. 2097 - 2105

Microemulsion assisted sol-gel procedure for nanostructured C_{60} silica – based materials synthesis

M. MIHALY*, A. ROGOZEA[a], A. COMANESCU, E. VASILE[b], A. MEGHEA
University Politehnica Bucharest, Faculty of Applied Chemistry and Materials Science, 1 Polizu, 011061, Bucharest, ROMANIA
[a]*ILIE MURGULESCU Institute of Physical Chemistry of the Romanian Academy, 202 Splaiul Independentei, 060021, Bucharest, ROMANIA*
[b]*METAV Research&Development, 020011, 31 C.A. Rosetti, Bucharest, ROMANIA*

Hybride C_{60} – silica based materials have been synthesized by microemulsion assisted sol – gel procedure. In this respect, the versatility of these soft – nanotechnologies has been exploited in order to obtain various type of nanostructures, such as C_{60} – silica coated nanoparticles and C_{60} – silica based composites The size, morphology and distribution of fullerene within the silica matrix, in liquid/solid phase, have been evaluated by adequate techniques: DLS, HR-TEM/SAED, XRD, BET. The size effect, photostability and semiconducting properties (band gap values) of the materials obtained have been quantified by means UV-VIS-NIR diffuse reflectance spectra. By corroborating these physico – chemical characteristics it can be concluded that these C_{60} – silica based hybride nanomaterials are promising in applications as optical devices, light-induced charge separation, semiconductors, chemical sensors, catalysis and in the medical field.

(Received September 2, 2010; accepted October 14, 2010)

Keywords: C_{60} – silica based nanomaterials, Sol-gel microemulsion, Photostability, Semiconductor

1. Introduction

Fullerene, C_{60}, is a promising material since such molecules have been shown to have remarkable physical and chemical properties – as good electron and free radical scavengers [1] that have prompted their use in photovoltaic cells [2], optical limiting solid-state devices (laser safety glasses) [3], non-linear optical devices [4, 5, 6], chemical sensors, energy storage [7-9], catalysis and photocatalysis [10,11] and the medical field [12-14]. The fullerene C_{60} molecules usually are characterized by a very low solubility, especially in polar solvents, thermal instability and tendency to form polydisperse microclusters [15], therefore their applications is restricted up to a greater extent. These applications are possible by hosting the fullerenes in a organic/inorganic matrices, such as polymers, metals, and ceramics [6, 16-18].

Silica matrix, an inorganic polymer, is not only thermally stable but durable and can be easly synthesized by sol-gel route [19].The use of silica materials as host matrices for fullerenes is advantageous since the molecules can be entrapped and covalently linked in the growing three-dimensional gel network having a high environmental stability and the final products show good chemical durability compared to polymers [20, 21].

Sol-gel processing is a successful route for C_{60} – silica hybrid materials synthesis and may lead to the development and durable final products [22,23,24]. However, even a flexible wet chemistry synthesis, such as sol-gel technique, encounters several limitations in the preparation of materials with a fine and homogenous dispersion of fullerenes. By using a microemulsion template [25 - 29] for sol-gel synthesis one can control the size, shape and distribution of fullerene molecules into the final material [30]. The microemulsion template can maintain or enhance the physico-chemical properties of fullerenes and can also overcome some of the obstacles in the application in materials science, such as the low fullerene solubility and their ability to aggregate, which further reduces the quality of the final product. Thus, the property of C_{60} to aggregate can be controlled when using a specific microemulsion template.

Consequently, the combination of sol-gel classic procedure and microemulsion template seems to be a versatile tool to prepare fullerene based nanocomposites materials [31,32]. Moreover, the microemulsion assisted sol-gel procedure can be also used at low temperatures of processing. In this way various silica based materials doped with fullerenes can be obtained by well controlling synthesis parameters.

In the present paper the preparation and characterization of the C_{60} – silica coated nanoparticles and C_{60} silica based composite materials are performed by using the microemulsion assisted sol-gel technique. The reasons for this work are as follows: i) to synthesise hybrid C_{60} – silica nanometer size structures that have potential applications in opto–electronics, semiconductors, catalysis, gas separations, chemical sensors and in the medical field as imaging probes, antioxidants and drug carriers; ii) to develop and demonstrate the versatility of the microemulsion assisted sol-gel procedure for the synthesis of new hybrid materials.

2. Materials and methods

2.1 Raw materials

All the chemicals were used as received. Tetraethoxysilane (TEOS), (1,1,3,3-tetramethylbutyl) phenyl-polyethylene glycol (TX-114), toluene,

dichlorobenzene, ethyl acetate (EtAc), acetonitrile (ACN), acetone were purchased from SIGMA-ALDRICH, fullerene (C_{60}) (99.9% purity) was obtained from Materials Electronics Research Corp. (MER) Corporation, pinus oil (P.O.) from FARES BIO VITAL Laboratories, Romania, hydrochloric acid (37%), potassium hydroxide (6M), ammonia solution 25% (NH_4OH) were purchased from MERCK. Ultra-pure water (Millipore Corporation) was used.

2.2. Preparation methods

Fullerene C_{60} nanoparticles as uncoated nanoclusters (C_{60} NP) (Fig. 1(a)), C_{60} nanoclusters embedded in silica matrix (C_{60}/SiO_2 bulk) (Fig. 1(b)) and silica coated C_{60} nanoparticles (C_{60}/SiO_2 NP) (Fig. 1(c)) have been synthesized by using oil in water (O/W) microemulsion template (Winsor IV) based on a TX-114/Pinus oil/Acetonitrile/Water system.

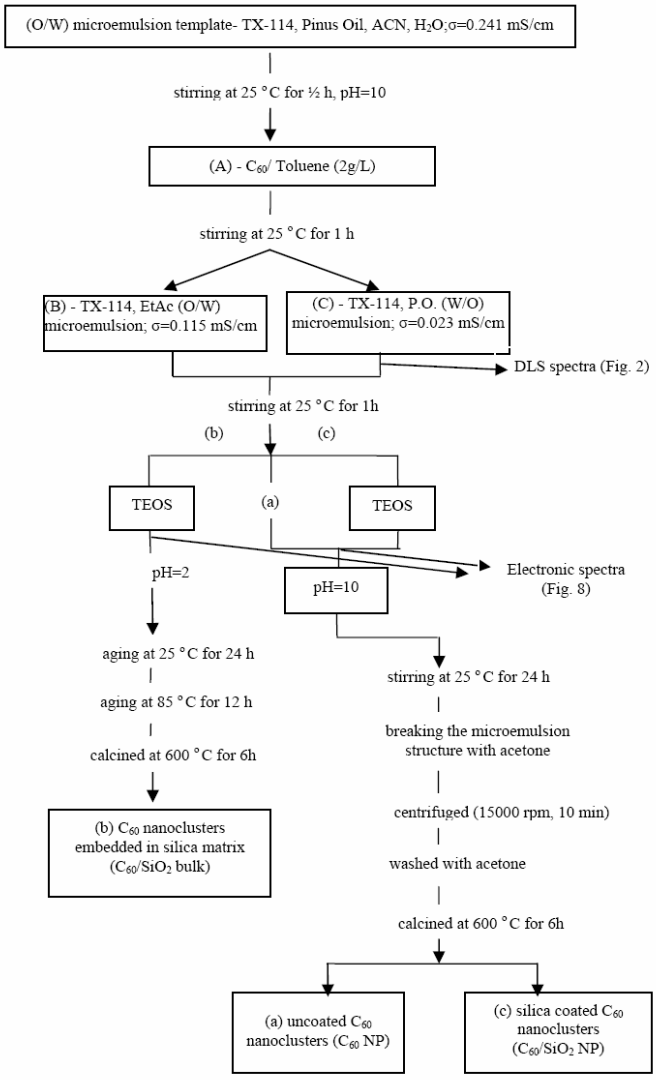

Fig.1. Schematic diagram for synthesis of the C_{60} NP (a), C_{60}/SiO_2 bulk (b) and C_{60}/SiO_2 NP (c)

The microemulsion O/W type (oil droplets dispersed in aqueous phase) is supported by the value of its electrical conductivity (σ = 0.241 mS/cm) After half an hour of stirring at room temperature a proper quantity of C_{60} in toluene solution (2g/L) was added maintaining the microemulsion aspect and properties (similar σ value). The concentration of fullerene in this system is of 0.01 %. This system is denoted by A. When to this system A a solution of TX-114 in EtAc is added (system B), the W/O microemulsion type is maintained (σ = 0.115 mS/cm). Separately, the system A was slowly poured into the TX-114 in Pinus oil solution previous prepared (system C) and the final mixture was stirred for another hour at room temperature. One can notice that the microemulsion type has been change from O/W to W/O, as it is confirmed by different values of electrical conductivity (σ = 0.241 mS/cm to σ = 0.023 mS/cm). Further, a method that combines microemulsion and sol-gel procedure has been used in the synthesis. The fullerene content in the silica matrix and in the silica coated nanoparticles is of 0.04 %

(w/w), respectively 0.12 % (w/w). In this type of syntheses, the organic precursor, TEOS, was added to the microemulsion bulk at a controlled pH, as shown in Fig. 1. The C_{60}/SiO_2 bulk thin film was deposited on a glass substrate by dip-coating method. After deposition, the film was firstly dried for 24 h at 25°C and then for 12 h at 85°C. The final materials were calcined at 600 ^oC for 6 hours in static conditions with a heating rate of 1 ^oC per minute, in order to eliminate all the organic residues.

2.3. Instruments and characterizations

The size estimation of the microemulsion systems applied as templates for the three types of C_{60} nanoclusters before their processing to final solid state was performed based on Dynamic Light Scattering (DLS) measurements on a Zetasizer Nano ZS, Malvern Instruments, UK. The size, shape and crystallinity of the calcined samples have been observed by High Resolution Transmission Electron Microscopy equipped with a Surface Area Electron Diffraction system (HR-TEM-SAED) realized on a PHILIPS CM 120 ST HR-TEM. Powder X-ray diffraction (PXRD) patterns were recorded on a X'Pert PRO PANalytical diffractometer equipped with a rotating anode and *Cu K α* radiation. Nitrogen adsorption measurements were conducted on a Quantachrome NOVA 2000 instrument at 77 K using a static adsorption procedure. The linear part of the Brunauer - Emmet - Teller (BET) equation (relative pressure (P/P_o) between 0.05 and 0.35) was used for the determination of the specific surface area. The spectral characterization of C_{60}/silica materials, as powders, was carried out by diffuse reflectance UV-VIS-NIR measurements on a JASCO V-550 Spectrophotometer equipped with an integrating sphere. Photostability experiments were carried out in an irradiation device, Bio-Sun from Vilbert Lourmat Company at UVA (365 nm) and UVB (312 nm) for the samples in solid phase.

3. Results and discussion

3.1 Size estimation of C_{60} nanoclusters dispersed in microemulsion phase

The fullerene nanoclusters are firstly characterized by using dynamic light scattering measurements.

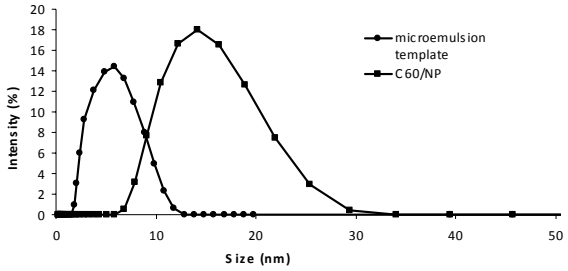

Fig. 2. Size estimation of the nanostructurated aggregates: the O/W microemulsion template and system A – C_{60}/NP by DLS measurement

The average diameter of the microemulsion droplets and that of C_{60} nanoclusters was 5.81 and 14.11 nm, respectively (Fig. 2) and both these samples showed a rather narrow cluster size distribution (polydispersity, Pld = 0.166. and 0.260), this confirming the high degree of homogeneity of these nano-dispersed systems. In order to understand the shape of the clusters of fullerene species, TEM studies were further carried out.

3.2 Topographic structure of calcined SiO_2 and C_{60}/silica materials

The morphology and distribution of fullerene within the silica matrix can be directly observed by High Resolution Transmission Electron Microscopy (HR-TEM). Typical silica particles prepared by microemulsion sol – gel procedure are illustrated in Fig. 3, which confirmed, by means of bright field transmission electron microscopy (TEM), the formation of silica spheres of about 30 nm in diameter with a uniform spherical morphology and without a particular pore shape or ordering within the silica spheres. These features were confirmed by the corresponding Selected Area Electron Diffraction image, (inset of Fig. 3), which suggests that the amorphous silica nanoparticles have been prepared.

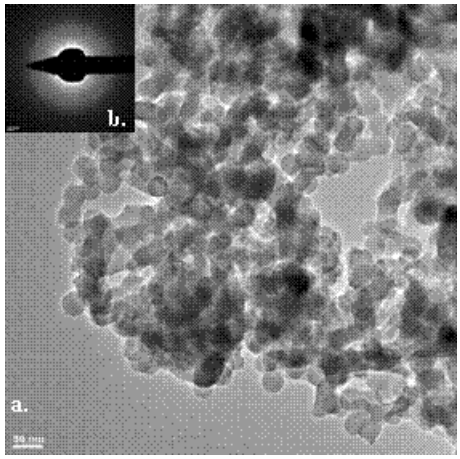

Fig. 3. High resolution transmission electron microscopy (HR-TEM) images of; a) SiO_2 bulk; b)the inset shows the corresponding SAED pattern of SiO_2 bulk

HR-TEM images of the fullerene molecules and fullerene uncoated nanoclusters, deposited on carbon grid are shown in Fig. 4.

Fig. 4(a) illustrates that the fullerene used in the synthesis is a Buckminsterfullerene with a spherical molecular structure where the carbon atoms are positioned at the vertices of a regular truncated icosahedron structure with 20 hexagons and 12 pentagons [33]. The diameter of a single molecule of C_{60} is 0.7 nm. The confirmation of fullerene nanoclusters is provided by the HR-TEM images shown in Fig. 4(b). From this figure, the size of the C_{60} clusters can be estimated to be around 10 nm.

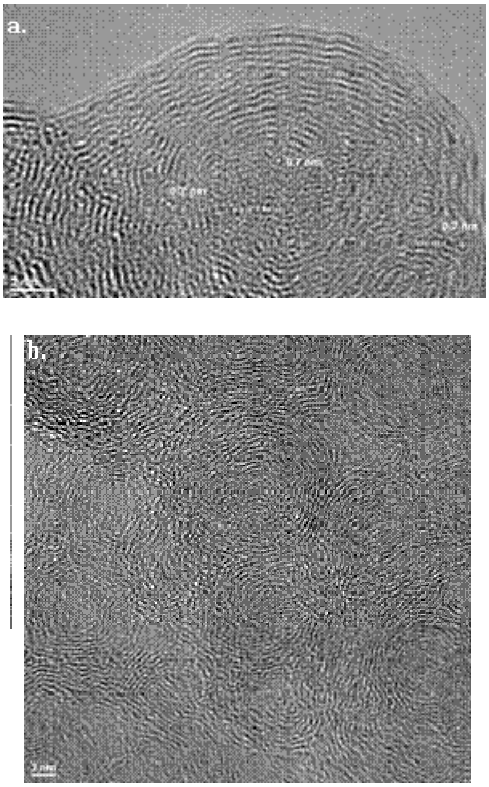

Fig. 4. High resolution transmission electron microscopy (HR-TEM) micrographs of (a) fullerene and (b) fullerene uncoated nanoclusters

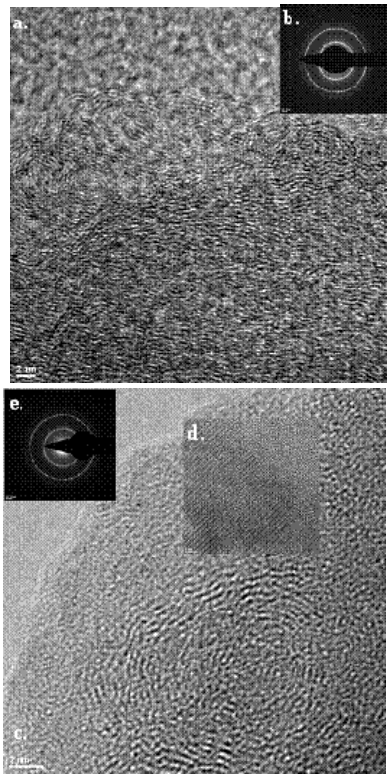

Fig. 5. High resolution transmission electron microscopy (HR-TEM) images of; a) C_{60} embedded in silica matrix; b)the inset shows the corresponding SAED pattern of C_{60}/SiO_2 bulk; c) C_{60} coated nanoclusters; d) the structure of mesoporous silica matrix; e) SAED patterns recorded on a single C_{60} coated nanocluster at a camera of 80 cm.

Fig. 5(a) shows the HR-TEM images of the C_{60} molecules embedded in silica matrix after calcination, which indicated wormhole like structures without a specific ordering. Selected area electron diffraction (SAED) was further performed on individual C_{60} nanoclusters embedded in silica matrix to investigate their structural ordering.

From Fig. 5(c), it can be observed that fullerene clusters are in the size range of 10-15 nm, and are exclusively confined inside the silica structure.

The nanoclusters of fullerene consist in several concentric layers with a polyhedral core and a spheroidal outer region. Although the inner shells of the particle can be seen to follow the shape of the core very closely, the shells become more spherical with increasing distance from the center of the particle as the ratio of the major to the minor diameter decreases toward unity.

The SAED patterns recorded at a camera length of 80 cm (Fig. 5(b, e)) consisted of a number of diffraction spots arranged in circular rings, indicating some areas of crystalline structures of silica induced by the ordered structures of fullerene nanoclusters. Also some amorphous structure is observed for silica matrix that surrounds the fullerene nanoclusters (Fig. 5(d)).

In the XRD patterns of solid C_{60} embedded in silica matrix (Fig. 6) and C_{60} SiO_2 coated nanoparticles (Fig. 7) different forms of silica could be detected such as: quartz, tridymite, cristobalite (polymorphs of quartz) (all are crystalline structures), silicon oxide (amorphous structure), and traces of fullerene (ordered structures). These results are confirmed by HR-TEM measurements.

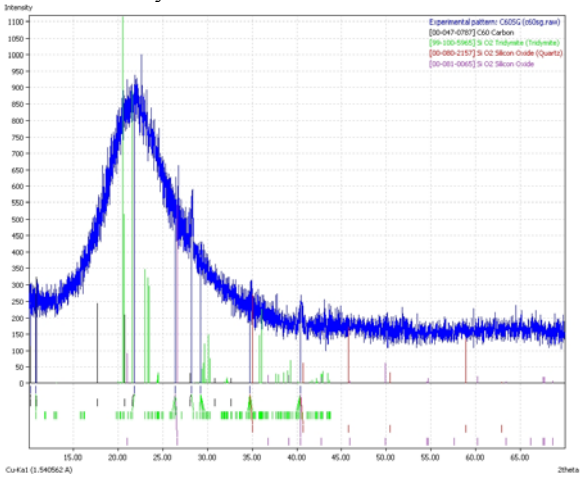

Fig. 6. XRD patterns recorded for the solid C_{60}/SiO_2 solid bulk.

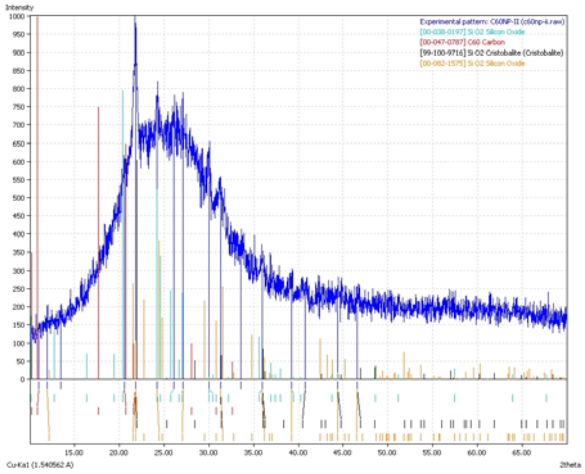

Fig. 7. XRD patterns recorded for the solid C_{60}/SiO_2 NP.

3.3. Textural properties of C_{60} – silica based materials

The surface areas of C_{60}/SiO_2 nanoparticles were determined by nitrogen adsorption at 77 K using BET method (Table 1). The calcined C_{60}/silica material shows a slightly higher BET surface area, 404 m^2/g^{-1}, compared to that of the silica matrix itself, 397 m^2/g^{-1}, suggesting that the fullerene molecules contributed some how to increase the adsorption capacity.

Table 1. The specific surface areas (A) of the prepared materials.

Sample	A (m^2/g)
SiO_2 bulk	397
C_{60}/SiO_2 bulk	404
C_{60} NP	4
C_{60}/SiO_2 NP	1
C_{60}	0.92

The absence of the inner channel structure within nanoparticle type materials is confirmed by lower specific surface areas of two magnitude orders for C_{60} NP and C_{60}/SiO_2 NP samples as compared to corresponding materials in bulk.

3.4. Spectral characterization of C_{60} – silica based materials

The electronic spectra of all types of C_{60}–based materials, both on liquid or solid samples, have been recorded in order to obtain valuable insights on their structural characteristics.

The UV-VIS spectra of microemulsion systems further used to prepare C_{60} nanoclusters, C_{60} nanoclusters embedded in silica and coated nanoparticles are presented in Fig. 8.

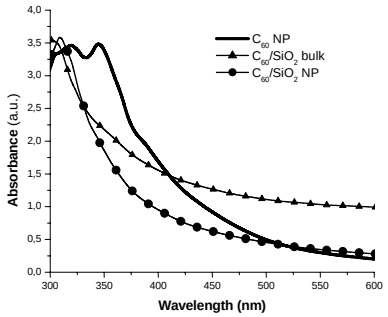

Fig. 8. The electronic spectra of the C_{60} NP (a), C_{60}/SiO_2 bulk (b) and C_{60}/SiO_2 NP (c) dispersed in microemulsion systems in liquid phase before the thermal treatment

As can be noticed, the C_{60} nanoclusters possess four well-separated bands, with absorption maxima at 304, 319, 345 and 390 nm, the last band being as a shoulder. This spectral pattern is characteristic to fullerene clusters in visible domain, which confers to the microemulsion system a yellow amber colour. This is different from the pristine violet colour of fullerene solution dissolved in toluene, with a broad absorption band between 450 – 650 nm and specific peaks around 575 nm ($\varepsilon \approx 10^3$) and 605 nm. Due to the micelle structure of microemulsion systems, the UV domain bellow 300 nm cannot be exploited; however, this blue shift of visible absorption band in fullerene clusters compared to its C_{60} monomer is conclusive for the aggregation process used to prepare controlled sized nanoclusters [34].

As referring to the other two spectra of microemulsion systems used to prepare C_{60} embedded in silica bulk and C_{60} coated nanoparticles, the absorption in visible domain is drastically diminished because of smaller concentration of the clustered chromophore, without visible peaks, but still with important absorption after 350 nm. This spectral behaviour sustains light yellow color specific to C_{60} clusters, now diluted by silica matrix in bulk or coating.

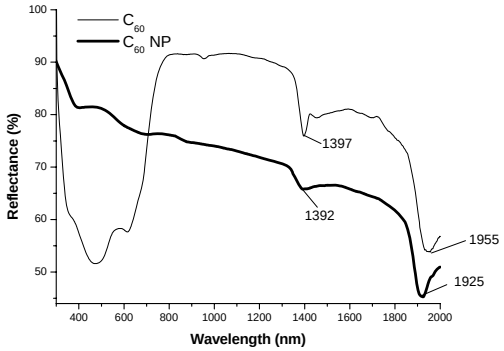

Fig. 9. VIS-NIR diffuse reflectance spectra of the solid C_{60} and C_{60} NP

The VIS-NIR diffuse reflectance spectra of pure C_{60} and C_{60} nanoclusters as powders, shown in Fig. 9, revealed similar features for these materials, by possessing a lower

absorption on the left part of visible domain (400 – 600) due to a lower chromophore content, and higher on the right part of visible and near infrared domains: 700 – 800 and 1400 – 2000 nm, as a result of aggregation (Table 2).

If compare VIS-NIR spectra of C_{60} silica coated and uncoated nanoparticles (Fig. 9, 10) it can be noticed that the absorption of coated nanoparticles is higher in visible domain and similar in NIR region, as is interpreted further.

Table 2. The specific wavelength measured in UV-VIS-NIR range for all the studied systems.

Sample	λ_1	λ_2	λ_3	λ_4	λ_5	λ_6	λ_7	λ_8	λ_9	λ_{10}	λ_{11}	λ_{12}	λ_{13}	λ_{14}
C_{60}	208	270	332	473		614		954			1397	1453	1955	
C_{60} NP	222	264	319	403		703					1392		1925	
SiO_2 NP		250									1389		1922	
C_{60}/SiO_2 NP	216	274	309		505		829			1212	1398		1927	
C_{60}/SiO_2 bulk	214	271	319			717	875	946	1152	1237	1405		1919	2220
C_{60}/SiO_2 bulk irradiated	209	270	317							1237	1376	1400	1909	2210
SiO_2 bulk			303			716	876	939	1149	1236	1376		1905	2215
SiO_2 bulk irradiated			313							1236	1376	1400	1906	2216

Table 3. The changes in ΔE, L, and the number of C_{60} molecules that form a cluster in the C_{60}-doped silicon materials.

Systems	λ_1 (nm)	λ_2 (nm)	$\Delta E\ 10^{22}$ (J)	The size of the C_{60} clusters L (nm)	The number of C_{60} forming a cluster [35]
C_{60}NP - C_{60}	1925	1955	15.84	10.67	438
C_{60}/SiO_2 NP - SiO_2/NP	1922	1927	2.68	25.9	6302
C_{60}/SiO_2 bulk - SiO_2 bulk	1905	1919	7.6	15.4	1317

Since NIR spectral domain is usually responsible for intermolecular interactions, by hydrogen bonds or charge transfer effects, it is reasonable to be used in quantifying the aggregation process. In this respect, three pairs of systems have been selected and compared in the Fig. 9, 10, 11, in order to estimate the cluster dimensions based on size effect of fullerene [35]: C_{60} nanoparticles referred to C_{60} monomer, C_{60} /SiO_2 nanoparticles referred to SiO_2 nanoparticles, and C_{60}/SiO_2 bulk referred to SiO_2 bulk matrix. It is worthwhile to mention that in each pair an appropriate reference material has been selected: pure fullerene, silica nanoparticles, and silica in bulk, respectively. The parameters used for calculus and the results obtained for cluster diameters and number of C_{60} molecules that form a cluster are collected in the Table 3.

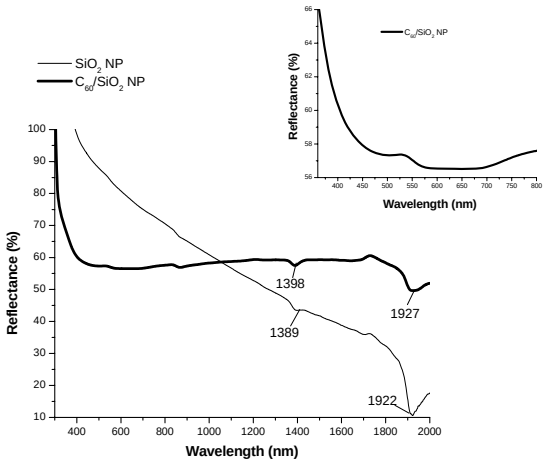

Fig. 10. VIS-NIR diffuse reflectance spectra of the SiO_2 NP and SiO_2 coated C_{60} NP (C_{60}/SiO_2 NP)

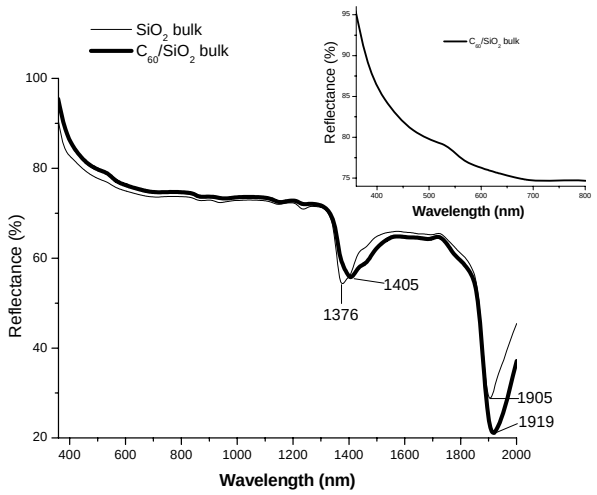

Fig. 11. VIS-NIR diffuse reflectance spectra of the SiO_2 bulk and C_{60}/SiO_2 bulk materials.

First of all it is remarkable to underline the agreement of C_{60} cluster size with that initially estimated by DLS and TEM measurements. Another observation is that the highest clusters are obtained for SiO_2 coated fullerene, this providing the explanation for the highest absorption in visible domain of this type of aggregated chromophore. This additional aggregation in coated C_{60} nanoparticles as compared to fullerene in the bulk silica could be produced during calcination process as a result of rather restricted available volume within rigid silica bulk matrix for the last material. Moreover, most of structural and morphological characteristics are similar for C_{60} NP and C_{60}/SiO_2 bulk, and quite different for silica coated fullerene, thus conferring the high versatility of microemulsion – sol gel procedure for various applications.

3.5. The photostability of silica based materials

In order to prepare silica based materials useful in applications such as light – induced charge separation or solar energy conversion, the use of fullerene doped silica materials, with large absorption of light almost on the entire visible domain, seems to be promising materials. However, it should be also demonstrated the photostability of this type of materials. In this respect, fullerene doped in silica bulk has been selected to be irradiated and compared with silica bulk as reference material.

The VIS-NIR diffuse-reflectance spectra of these silica and C_{60}/silica doped materials before and after irradiation are illustrated in Fig. 12 for visible (a) and NIR (b) domains. One can notice that the general pattern of spectra remains practically unchanged, without significant shifts in peak wavelengths. However, the intensity of silica bulk reflectance is drastically increased, the higher transparency of the silica matrix probably being the result of its conversion from amorphous to crystalline form. In similar conditions of irradiation (time = 3 h, UVA energy 50J/cm^2, UVB energy 25J/cm^2) the intensity of reflectance remained almost the same in irradiated C_{60}/silica doped samples compared to non-irradiated sample, thus demonstrating the high photostability induced by fullerene doping to silica matrix, and their potential applications in photovoltaics or photocatalysis.

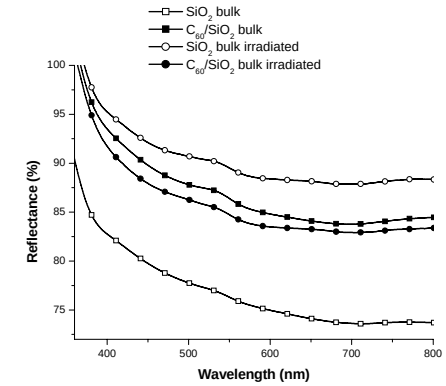

a

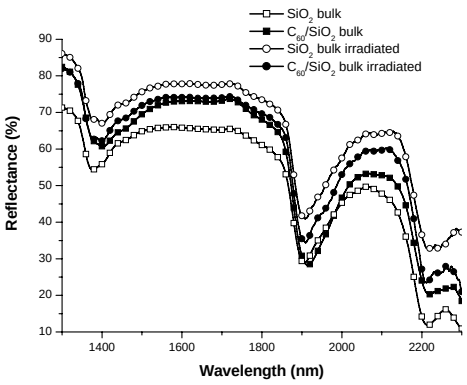

b

Fig. 12. VIS-NIR diffuse-reflectance spectra of the SiO_2 bulk and C_{60}/SiO_2 bulk materials before and after irrirradiation (a) the VIS scale, b) only the NIR scale

3.6. Semiconductor properties of C_{60} silica based materials

It is well known that fullerene belongs to a series of carbon compounds composed only of carbon atoms, similar to diamond and graphite. Since the fullerene was firstly obtained in 1999 by arc discharge of a carbon electrode it was also considered as a carbonaceous semiconductor material [36,37].

Table 4. Energy band gap distribution for the prepared materials.

Sample	Energy band gap (eV)
C_{60}	1.87
C_{60} solid NP	2.4
C_{60}/SiO_2 solid NP	3.07
C_{60}/SiO_2 solid bulk	3.04

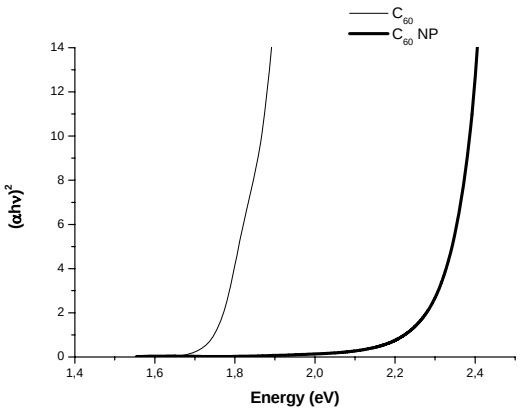

Fig. 13. Energy band-gap determinations of C_{60} and C_{60} NP

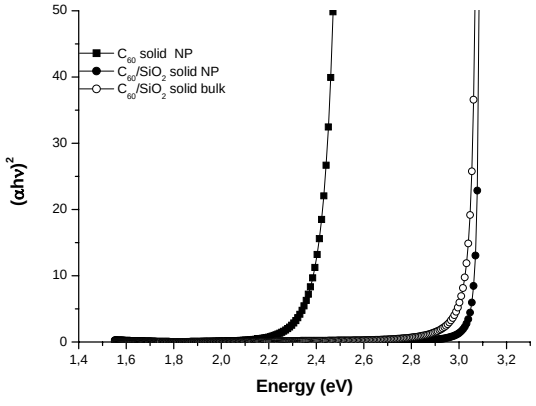

Fig. 14. Energy band gap determination of C_{60}NP, C_{60}/SiO_2 NP, C_{60}/SiO_2 bulk in solid phase

In the crystalline form of C_{60} the molecules are arranged in a face-centered cubic structure. It exhibits a band gap of 1.8 eV (Fig. 13) and may be deemed as a semiconductor. After incorporating the C_{60} nanoparticles (2.4 eV) (Table 4) into a silica matrix, two types of semiconductors with similar band gaps around 3 eV have been obtained (Fig. 14).

The energy band gap of these materials is determined by the reflection spectra, according to the Tauc relation [38,39]. In this way, new C_{60} silica based nanostructured materials, as stable catalysts, could be prepared, able to absorb light on the entire visible range of the spectrum.

4. Summary

Three different types of C_{60} based materials have been synthesized, C_{60} nanoclusters, silica coated, and silica embedded, *via* a microemulsion assisted sol-gel procedure. For the synthesis of C_{60} nanoclusters embedded in silica matrix, the oil in water microemulsion of pinus oil/TX-114/aqueous phase was used, while for C_{60}/SiO_2 coated nanoparticles water in oil microemulsion was prepared.

The microemulsification represents a unique method for obtaining the monodispersed fullerene nanoclusters. This is the first stage of the preparation of hybrid nanocomposites based on formation of the silica network around the molecules within the microemulsion colloidal aggregates.

The microemulsion assisted sol –gel procedure developed by this study has some important highlights as:

- the ability of microemulsion to inverse the organic phase, where the nanoparticles are synthesized, to inorganic one, corresponding to silica matrix.

- the possibility to control the size and shape of nanoparticles and to avoid their aggregation resulting into an high degree of homogeneity and monodispersity of the final materials.

- the accessibility of every important synthesis step for a proper characterization method that allows obtaining of pre-designed materials.

- the suitability for hybrid nanomaterials synthesis (uncoated/coated nanoparticles, bulk, and thin film).

The structural properties of native C_{60} nanoclusters, as shown by VIS-NIR spectroscopy, TEM and AFM microscopy, XRD measurements, are revealed in all the three types of materials synthesized by microemulsion assisted sol-gel method.

The higher specific surface area of silica bulk materials and their photostability by doping with C_{60} nanoclusters, suggesting increased adsorption efficiency, recommends testing them for separation properties.

Semiconductor materials have been obtained (1.8 ÷ 3 eV) which may be evaluated as potential catalysts, as the amorphous silica constitutes a novel type of catalysts support because of its porous structure, high thermal stability, optical transparency and chemical inertness.

These hybrid materials may have applications in areas as optical devices, light-induced charge separation,

semiconductors, chemical sensors, catalysis and in the medical field.

Acknowledgements

The work has been funded by the Sectorial Operational Programme Human Resources Development 2007-2013 of the Romanian Ministry of Labour, Family and Social Protection through the Financial Agreement POSDRU/6/1.5/S/19.

References

[1] C.H. Lee, T.S. Lin, H.P. Lin, Q. Zhao, S.B. Liu, C. Y. Mou, Microporous Mesoporous Mater. **57,** 199 (2003).
[2] A.Kohler, H.F. Wittmann, R.H. Friend, M.S. Khan, J. Lewis, Synth. Met. **77**, 147 (1996).
[3] R. Signorini, M. Zerbetto, M. Meneghetti, R. Bozio, M. Maggini, C. De Faveri, M. Prato, G. Scorrano, Chem. Commun. 1891 (1996).
[4] F. M. Li, Makromol. Symp. **101**, 227 (1996).
[5] N. S. Sariciftici, A.J. Heeger, Proc. SPIE-Int. Soc. Opt. Eng. **2530**, 76 (1995).
[6] S. V. Patwardhan, N. Mukherjee, M. F. Durstock, L. Y. Chiang, S.J. Clarson, J. Inorg. Organomet. Polim., **12**, 49 (2002).
[7] Y. Ju-Nam, J.R. Lead, Sci. Total Environ. **400**, 400 (2008).
[8] D. H. Yang, C. S. Park, J. H. Min, M. H. Oh, Y. S. Yoon, S. W. Lee, J.S. Shin, Curr. Appl Phys. **9**, 133 (2009).
[9] F. Augusto, E. Carasek, R. G. Costa Silva, S. R. Rivellino, A.D. Batista, E. Martendal, J. Chromatogr. A **1217**, 2536 (2010).
[10] P. R. Mishra, O. N. Srivastava, Bull. .Mat. Sci. **31**, 545 (2008).
[11] M. D. Tzirakis, J. Vakros, L.A. Loukatzikou, V. Amargianitakis, M. Orfanopoulos, C. Kordulis, A. Lycourghiotis, J. Molecular Catalysis A: Chemical **316**, 65 (2010).
[12] R. M. Baum, C&EN **71**, 8 (1993).
[13] N. Levi, R. R. Hantgan, M. O. Lively, D. I. Carroll, G. L. Prasad, J. Nanobiotechnology **4**, 14 (2006).
[14] J. Jeong, M. Cho, Y.T. Lim, N.W. Song, B.H. Chung, Angew. Chem. **121**, 5400 (2009).
[15] R.V. Bensasson, E. Bienvenue, M. Dellinger, S. Leach, P. Seta, J. Phys. Chem. **98**, 3492 (1994).
[16] P. Innocenzi, G. Brusatin, Chem. Mater. **13**, 3126 (2001).
[17] E.A. Whitsitt, A.R. Barron, Chem. Commun. (2003) 1042.
[18] L. Zhu, P.P. Ong, J. Shen, J. Wang, J. Phys. Chem. Solids **59**, 819 (1998).
[19] C. J. Brinker, G. W. Scherer, Sol-Gel Science: The Physics and Chemistry of Sol-Gel Processing; Academic Press, 1990.
[20] M. Meneghetti, R. Signorini, M. Zerbetto, R. Bozio, M. Maggini, G. Scorrano, M. Prato, G. Brusatin, E. Menegazzo, M. Guglielmi, Synth. Met. **86**, 2353 (1997).
[21] L. Zhu, Y. Li, J. Wang, J. Shen, Chem. Phys. Lett. **239**, 395 (1995).
[22] G. A. Ozin, A. C. Arsenault, L. Cademartiri, Nanochemistry; The Royal Society of Chemistry, 2009.
[23] G. Brusatin, P. Innocenzi, J. Sol-Gel Sci. Technol. **22**, 192 (2001).
[24] H. Peng, J. W. Y. Lam, F. S. M. Leung, T. W. H. Poon, A. X. Wu, N. T. Yu, B. Z. Tang, J. Sol-Gel Sci. Technol. 22, 205 (2001).
[25] C. Stubenrauch, Microemulsion, Wiley-VCH, 2009.
[26] J. Ahmed, S. Sharma, K. V. Ramanujachary, S. E. Lo, A. K. Ganguli, J. Colloid Interface Sci. **336**, 814 (2009).
[27] T. Aubert, F. Grasset, S. Mornet, E. Duguet, O. Cador, S. Cordier, Y. Molard, V. Demange, M. Mortier, H. Haneda, J. Colloid Interface Sci. **341**, 201 (2010).
[28] H. Zhang, X. Wang, D. Wu, J. Colloid Interface Sci. **343**, 246 (2010).
[29] M. N. Luwang, R. S. Ningthoujam, N. S. Singh, R. Tewari, S. K. Srivastava, R. K. Vatsa, J. Colloid Interface Sci. (2010), doi:10.1016/j.jcis.2010.05.037
[30] M. Mihaly, A. Comanescu, A. Rogozea, C. Pirvu, I. Rau, Nanobiosystems: Processing, Characterization, and Applications II, Proc. SPIE-Int. Soc. Opt. Eng. **7403**, 740308 (2009).
[31] D. Vollath, Nanomaterials, Wiley-VCH, 2009.
[32] U. Schubert, N. Husing, Synthesis of Inorganic Materials; Wiley-VCH, 2000.
[33] H. W. Kroto, J. R. Heath, S. C. O'Brien, R. F. Curl, R. E. Smalley, Nature **318**, 162 (1985).
[34] Y. P. Sun, C. E. Bunker, B. Ma, B. Liu, J. Amer. Chem. Soc. **117**, 12709 (1995).
[35] I. Hasegawa, S. Nonomura, J. Sol-Gel Sci. Technol **19**, 300 (2000).
[36] M. Kusunoki, T. Watanabe, S. Yamamichi, M. Ata, S. Mizuno, M. Ramm, Patent US 6, 471, 929 B1, 2002.
[37] K. Sattler, in H.S. Nalwa (Ed.), Handbook of Thin Films Materials, Volume 5: Nanomaterials and Magnetic Thin Films Academic Press, 2002, p. 61.
[38] G.P. Joshi, N.S Saxena, R. Mangal, A. Mishra, T. P. Sharma, Bull. Mater. Sci., **26**, 387 (2003).
[39] D. Patidar, R. Sharma, N. Jain, T. P. Sharma, N. S. Saxena, Bull. Mater. Sci., 29 (2006) 21.

*Corresponding author: maria.mihaly@upb.ro